A high-pressure cryocooling method for protein crystals and biological samples with reduced background X-ray scatter

Chae Un Kim,[a]* Jennifer L. Wierman,[b] Richard Gillilan,[a] Enju Lima[c] and Sol M. Gruner[a,b,d]

[a]Cornell High Energy Synchrotron Source (CHESS) and Macromolecular Diffraction Facility at CHESS (MacCHESS), Cornell University, Ithaca, NY 14853, USA, [b]Field of Biophysics, Cornell University, Ithaca, NY 14853, USA, [c]Brookhaven National Laboratory, Upton, NY 11973, USA, and [d]Department of Physics, Cornell University, Ithaca, NY 14853, USA. Correspondence e-mail: ck243@cornell.edu

High-pressure cryocooling has been developed as an alternative method for cryopreservation of macromolecular crystals and successfully applied for various technical and scientific studies. The method requires the preservation of crystal hydration as the crystal is pressurized with dry helium gas. Previously, crystal hydration was maintained either by coating crystals with a mineral oil or by enclosing crystals in a capillary which was filled with crystallization mother liquor. These methods are not well suited to weakly diffracting crystals because of the relatively high background scattering from the hydrating materials. Here, an alternative method of crystal hydration, called capillary shielding, is described. The specimen is kept hydrated *via* vapor diffusion in a shielding capillary while it is being pressure cryocooled. After cryocooling, the shielding capillary is removed to reduce background X-ray scattering. It is shown that, compared to previous crystal-hydration methods, the new hydration method produces superior crystal diffraction with little sign of crystal damage. Using the new method, a weakly diffracting protein crystal may be properly pressure cryocooled with little or no addition of external cryoprotectants, and significantly reduced background scattering can be observed from the resulting sample. Beyond the applications for macromolecular crystallography, it is shown that the method has great potential for the preparation of noncrystalline hydrated biological samples for coherent diffraction imaging with future X-ray sources.

1. Introduction

It is now routine that macromolecular crystal structures are determined at cryogenic temperatures (∼100 K) to limit radiation damage during X-ray diffraction experiments (Dewan & Tilton, 1987; Garman & Schneider, 1997; Haas & Rossmann, 1970; Hope, 1988; Low *et al.*, 1966). However, the crystal cooling process typically leads to disruption of crystal order and, therefore, results in a decrease in diffraction quality. To overcome this problem, crystals are often soaked in a cryoprotective solution prior to cooling (Garman, 1999, 2003; Garman & Doublie, 2003; Garman & Owen, 2006; Haas & Rossmann, 1970; Henderson, 1990; Hope, 1988; Juers & Matthews, 2004; Kriminski *et al.*, 2002; Rodgers, 1994; Schneider, 1997; Alcorn & Juers, 2010; Bujacz *et al.*, 2010; Chinte *et al.*, 2005; Garman & Mitchell, 1996; Mueller-Dieckmann *et al.*, 2011; Petsko, 1975; Pflugrath, 2004; Rodgers, 1997; Warkentin *et al.*, 2006). However, finding the optimal cryoprotective conditions for a given crystal often requires substantial time-consuming screening.

A recent alternative to the conventional cryoprotection method is high-pressure cryocooling (Kim *et al.*, 2005). In this method, crystals are pressurized with helium gas to pressures in the 200 MPa range and then subsequently cooled quickly to liquid nitrogen temperature. This method minimizes or completely eliminates the need for added penetrative chemical cryoprotectants. During cryocooling at high pressure, the water within protein crystals turns into an unusual ice phase, high-density amorphous (HDA) ice, which is less disruptive to the crystal lattice than the low-density amorphous ice produced during ambient-pressure cryocooling (Kim *et al.*, 2005, 2008). It has been demonstrated that HDA ice is stable below 100 K, allowing high-pressure cryocooled protein crystals to retain pressure effects at cryogenic temperatures, even when restored to ambient pressure (Kim *et al.*, 2008). This observation enabled the use of high-pressure cryocooling for various important technical and scientific applications as described below.

High-pressure cryocooling was developed primarily for crystal cryoprotection and dozens of unique macromolecular

crystals have been successfully cryopreserved, including membrane protein crystals (*e.g.* a Kv ion channel; cytochrome c oxidase) and large RNA/protein complexes, such as the ribosome. The method was extended to anomalous diffraction phasing by incorporating noble gases such as Kr and Xe (Kim *et al.*, 2006, 2007). In addition, high-pressure cryocooling was successfully applied to stabilize ligand–protein interactions (Albright *et al.*, 2006) and to study the pressure effect on the structure of a yellow fluorescent protein, citrine (Barstow *et al.*, 2008, 2009). The procedure was then modified to entrap an intermediate enzymatic state of human carbonic anhydrase (Domsic *et al.*, 2008). More recently, the method was used to study the phase behavior of water inside protein crystals (Kim *et al.*, 2009) and its relationship with protein dynamics at cryogenic temperatures (Kim *et al.*, 2011).

The pressure cryocooling reported by Kim *et al.* (2005) involves coating protein crystals with mineral oil to prevent crystal dehydration (Kwong & Liu, 1999; Riboldi-Tunnicliffe & Hilgenfeld, 1999; Hope, 1988). Although this oil-coating method was successful for various different kinds of protein crystals, it is not appropriate for some protein crystals that are very fragile or unstable in oil. For those crystals, a different crystal-hydration method using a plastic capillary was developed (Kim *et al.*, 2007). In this capillary-hydration method, protein crystals are either grown or transferred into a plastic capillary and the crystals are hydrated with the solution in the capillary. Protein crystals hydrated either by oil coating or by capillary hydration produce good diffraction after pressure cryocooling (Kim *et al.*, 2007, 2005). However, both methods have an obvious drawback. The crystal-surrounding materials (oil or capillary and mother liquor solution) contribute a relatively high X-ray background. This background can obscure diffraction spots from very weakly diffracting crystals. To overcome this problem, we developed a new crystal-hydration method, called capillary shielding.

2. Materials and methods

2.1. Protein crystallization and crystal handling

The protein crystallization technique was a modified version of that described by Ko *et al.* (1994) and was performed as described by Kim *et al.* (2005, 2007). Lyophilized thaumatin powder from *Thaumatococcus daniellii* (Sigma, Saint Louis, MO, USA) was used for crystallization without further purification. For the oil-coating and capillary-shielding method, crystals were grown at 293 K by the hanging-drop method with 25 mg ml^{-1} of thaumatin solution in 50 mM HEPES buffer at pH 7 and a crystallization solution containing 0.9 M sodium potassium tartrate (NaK tartrate) as a precipitant. The crystal space group was determined to be $P4_12_12$ ($a = b \simeq 58$, $c \simeq 150$ Å), having a solvent content of 55–60% by volume. To exchange solvent in protein crystals from 0.9 M NaK tartrate to 10%(v/v) glycerol in deionized water, the fully grown thaumatin crystals were first equilibrated to 10% glycerol (v/v) in 0.9 M NaK tartrate solution and slowly

reduced to 0 M in 0.1 M steps, to minimize osmotic shock. The crystal sizes were *ca* 100 × 100 × 150 µm.

For the capillary-hydration method, thaumatin crystallization was carried out at 293 K in a polycarbonate capillary with an inside diameter of 200 µm and a wall thickness of 50 µm (Drummond Scientific Company, Broomall, PA, USA). Equal amounts of protein solution (25 mg ml^{-1} in 50 mM HEPES buffer pH 7.0) and reservoir solution containing 0.9 M NaK tartrate were mixed. The mixed solution was then inserted into the polycarbonate capillary and the capillary was placed into a 15 ml centrifuge tube containing 0.9 M NaK tartrate solution at the bottom. The large tube was carefully sealed with Parafilm to minimize evaporation of the crystallizing solution and the reservoir solution. Equilibrium between the capillary and the reservoir solution in the larger tube was reached by vapor diffusion. Crystals appeared within a few days and grew on the capillary inner surface (*ca* 75 × 75 × 100 µm in size) in a few weeks.

2.2. Crystal hydration methods

2.2.1. Oil coating and capillary hydration. The oil-coating and capillary-hydration methods were performed as described by Kim *et al.* (2005, 2007). In the oil-coating method, NVH oil (Hampton Research, Aliso Viejo, CA, USA) was directly applied to cover the mother liquor droplet containing the desired crystals on the coverslip from the hanging-drop crystallization tray. Crystals were gently dragged from the droplet into the oil. In the oil, crystals were swished back and forth to remove excess external mother liquor on the surface of the crystals. In this study, to estimate the crystal damage from physical handling, the external mother liquor was aggressively removed to the point that the crystal surface became slightly rough. The crystals were picked up in commercially available cryoloops (Hampton Research) with a minimal droplet of oil (Fig. 1*a*) and high-pressure cryocooled.

In the capillary-hydration method, the polycarbonate capillary containing crystals was cut to a length of ∼15 mm, and the entire capillary was high-pressure cryocooled. In the capillary, protein crystals were fully hydrated by the mother liquor solution. Both capillary ends were left open for pressure equilibration, but solution evaporation was negligible during high-pressure cryocooling (Fig. 1*b*).

2.2.2. Capillary shielding. In the capillary-shielding method, a protein crystal was picked up from a hanging droplet in a cryoloop. The crystal sample in the loop was then inserted into the open end of a shielding polyester capillary (outside diameter = 864 µm, wall = 25.4 µm; Advanced Polymers, Salem, NH, USA) containing a reservoir solution of the mother liquor at the opposite end (Fig. 1*c*). The opposite end was also left open, but mother liquor evaporation was negligible during high-pressure cryocooling. The shielding capillary was glued with 5 min epoxy to the loop post. The capillary was partially cut through to allow pressure equilibration during pressurization with helium gas. The sample was kept hydrated throughout the pressure cryocooling process *via* vapor diffusion from the solution reservoir in the capillary. A similar

approach to the capillary shielding was reported for crystal hydration and data collection at room temperature by Kalinin *et al.* (2005). After pressure cryocooling, the outside shielding capillary was removed before loading the sample onto a goniometer at the X-ray beamline (Figs. 1*d*–1*f*), with care taken never to let the crystal warm appreciably. Using the capillary-shielding method, the diffuse scattering background from sample-coating materials such as oil or an enclosing capillary and excess mother liquor could be eliminated.

To investigate a possible future application for the coherent X-ray diffraction imaging of noncrystalline biological materials, thin-solution films in nylon loops [10% glycerol solution (*v*/*v*), ~20 µm thickness] were high-pressure cryocooled using the capillary-shielding method. The ice phase induced in the solution film was then investigated by X-ray scattering.

2.3. High-pressure cryocooling

The hydrated crystals were high-pressure cryocooled as described by Kim *et al.* (2005). Briefly, crystals were loaded into a high-pressure cryocooling apparatus consisting of commercial high-pressure plumbing and pressure transducers. The apparatus containing the crystals was then pressurized with helium gas to 200 MPa pressure in 2 min and the crystal samples were equilibrated in pressure for 5 min. Afterwards, a magnetic constraint was released and the crystals fell down a length of high-pressure tubing into a cold zone kept at liquid N_2 temperature (77 K). The helium pressure was released and

the crystals were transferred to regular cryocaps in liquid nitrogen for data collection. After the procedure, the high-pressure cryocooled crystals can be handled at ambient pressure in the same manner as normal flash-cryocooled crystals for cryocrystallographic data collection. We found that the crystals were stable at ambient pressure for at least several months, retaining pressure effects as long as they were kept at liquid nitrogen temperature. Note that the crystal cooling rate using gas high-pressure cryocooling is much higher than that with the liquid high-pressure cryocooling method described by Urayama *et al.* (2002). In gas high-pressure cryocooling, protein crystals are cryocooled by immersion into compressed He gas, which is precooled to 77 K. We estimate that the cooling rate for an oil-coated crystal (~200 µm) is comparable to the cooling rate of flash cooling in an N_2 gas stream at ambient pressure (a few hundred kelvin per second) (Teng & Moffat, 1998).

2.4. Crystallographic data collection and processing

The X-ray diffraction data were collected at the macromolecular crystallography station F1 (λ = 0.9179 Å, Area Detector Systems Corporation Quantum 270 CCD detector, beam size of 100 µm) at the Cornell High Energy Synchrotron Source (CHESS). A complete data set was collected from each crystal at 100 K, covering 90° of crystal rotation. The X-ray exposure time was 1 s with an oscillation angle of 1°. In all cases the detector face was perpendicular to the incident beam
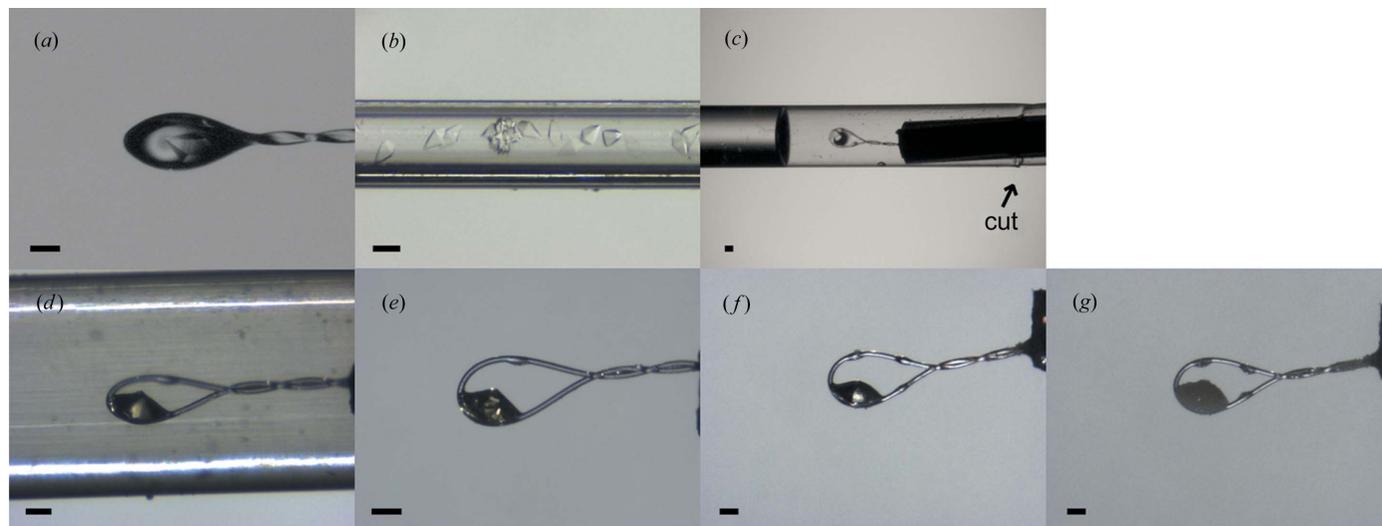
Figure 1
Three crystal-hydration methods for high-pressure cryocooling. The scale bar in each figure indicates 100 µm. (*a*) Oil-coating method. The method can remove excess mother liquor, which is helpful to suppress water crystallization inside crystals. The image was taken at room temperature before high-pressure cryocooling. (*b*) Capillary-hydration method. Crystals are grown in a capillary and are hydrated by the surrounding mother liquor. The image was taken on the beamline at 100 K after high-pressure cryocooling. (*c*)–(*f*) Capillary-shielding method. The crystal is picked up in a cryoloop and inserted into a polyester capillary which has a plug of mother liquor in the other end. (*c*) The crystal is hydrated by vapor diffusion between the mother liquor and the cryoloop. A small cut in the enclosing capillary facilitates pressure equilibration during pressure cryocooling. The image was taken at room temperature before high-pressure cryocooling. (*d*) The image of a capillary-shielded crystal on the beamline (100 K) after high-pressure cryocooling, with the polyester capillary still attached. (*e*) The crystal in (*d*) was transferred back to liquid nitrogen to remove the polyester capillary and then reloaded on the beamline (100 K). (*f*) Another crystal on the beamline (100 K) prepared by the capillary-shielding method. The crystal was equilibrated with 10%(*v*/*v*) glycerol solution (in deionized water) before high-pressure cryocooling. (*g*) The same crystal as in (*f*) was quickly warmed to room temperature and refrozen back to 100 K in a nitrogen gas stream. The crystal is swollen with bubbles because of the release of compressed He gas captured in the sample during high-pressure cryocooling.

and the sample-to-detector distance was 200 mm. The complete diffraction data sets were indexed, pre-refined, integrated, post-refined and scaled with *HKL-2000* (Otwinowski & Minor, 1997). The crystal mosaicity was obtained during the scaling process using *HKL-2000*. To properly compare processing statistics from different data sets, the same processing parameters were used for all data sets.

2.5. Small-angle X-ray scattering data collection and processing

A small-angle X-ray scattering (SAXS) experiment was performed to probe the homogeneity of the high-density amorphous ice produced by high-pressure cryocooling. The solution film ($\sim$10 µm) induced by the capillary shielding produced very weak SAXS signals. To increase the signal-to-noise ratio, a sample cell was constructed from a short section of polycarbonate capillary (outside diameter 914 µm, inside diameter 635 µm; Drummond Scientific Company, Broomall, PA, USA), mounted coaxially to the beam on the end of a steel pin with a Hampton-style magnetic base. In this configuration, the X-ray beam passed down the axis of the capillary tube through approximately 1 mm of frozen sample without encountering any window material. The $\sim$1 mm path length ensured a strong SAXS signal. 15%(v/v) glycerol solution was loaded into the capillary and high-pressure cryocooled at 200 MPa. SAXS data were collected on CHESS beamline G1 at 10.5 keV (1.18 Å) using multilayer optics with a bandwidth
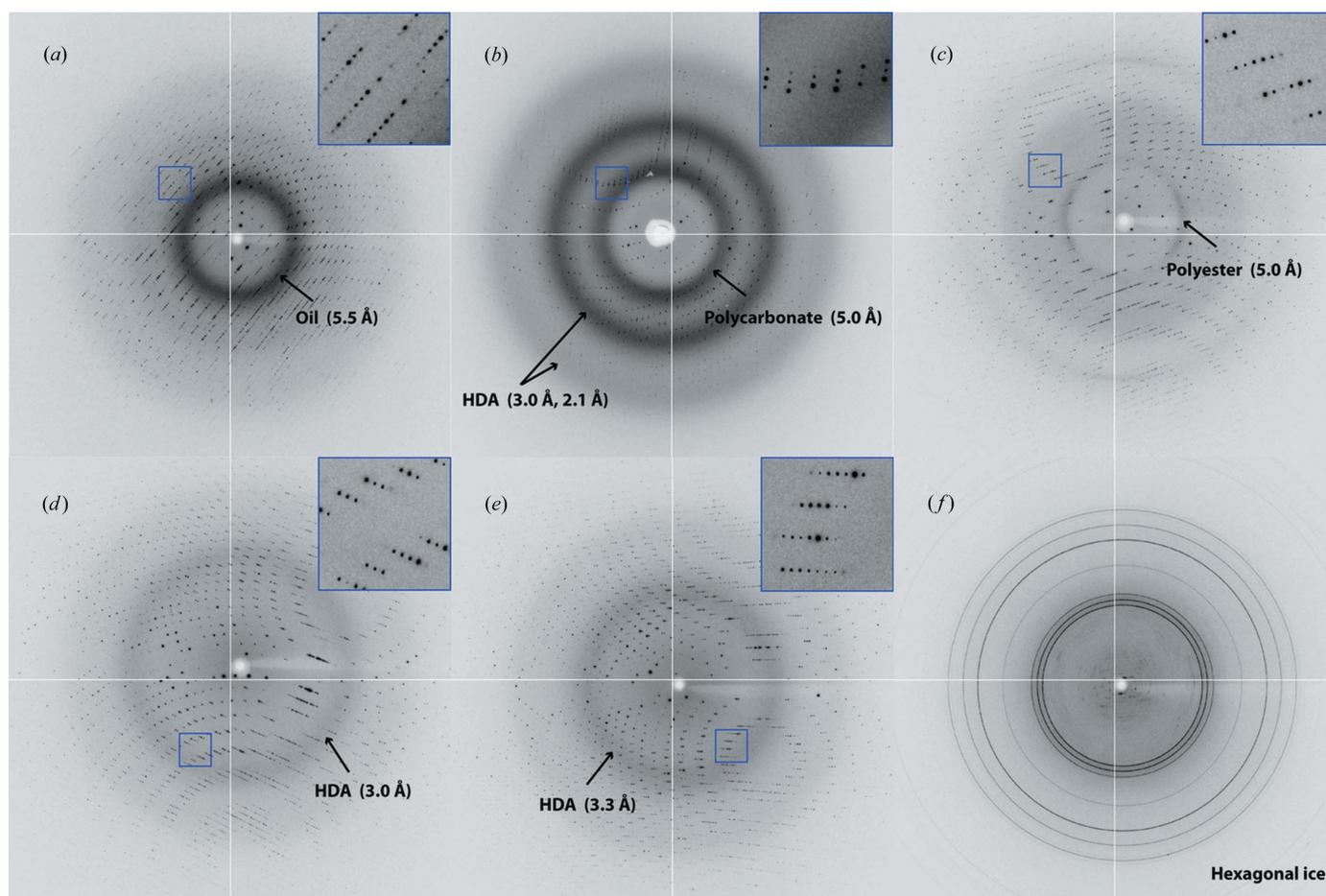
Figure 2
Diffraction images of high-pressure cryocooled crystals prepared by three hydration methods. (*a*) Oil-coating method (Fig. 1*a*). The image shows diffuse scattering at around 5.5 Å from oil. Crystal mosaicity is 0.67°. (*b*) Capillary-hydration method (Fig. 1*b*). The innermost diffuse ring ($\sim$5.0 Å) is generated from the polycarbonate capillary, and the second and third diffuse rings are from the solvent (HDA ice) inside the capillary. Crystal mosaicity is 0.34°. (*c*) Capillary-shielding method, but without removing the polyester capillary (Fig. 1*d*). Although the scattering from the polyester capillary is present (anisotropic peak at $\sim$5.0 Å), the background level is dramatically reduced compared to the oil-coating and capillary-hydration methods. Crystal mosaicity is 0.11°. (*d*) Capillary shielding with removal of the polyester capillary (Fig. 1*e*). The image shows faint diffuse scattering around 3.0 Å, which is from the small amount of external and internal solvent (HDA ice) in and around the crystal. Note that the level of diffuse scattering from the solvent is comparable to the air scattering around the beam stop. Crystal mosaicity is 0.12°. The slight increase in unit-cell dimensions and mosaicity from 0.11° (see Table 1) is due to X-ray radiation damage (Ravelli & McSweeney, 2000). (*e*) Crystal equilibrated to 10%(v/v) glycerol in deionized water (Fig. 1*f*), then prepared by the capillary-shielding method; the polyester capillary was removed before data collection. The diffuse scattering from the solvent (HDA ice) is shifted to 3.3 Å owing to the addition of glycerol and removal of NaK tartrate. Crystal mosaicity is 0.08°. (*f*) Diffraction image of the crystal after warming to room temperature and being refrozen to 100 K in the N_2 gas cold stream at the beamline at ambient pressure (Fig. 1*g*). It shows strong diffraction rings from hexagonal ice formation and very poor quality diffraction from the protein crystal. The result indicates that the crystal was kept hydrated during the capillary-shielding method.

Table 1
Data collection and processing statistics of thaumatin crystals prepared by three crystal-hydration methods.

Values in parentheses are for the highest resolution shell.

Protein	Thaumatin				
Hydration method	Oil coating	Capillary hydration	Capillary shielding, polyester capillary on†	Capillary shielding, polyester capillary off†	Capillary shielding, polyester capillary off
Solvent condition	0.9 M NaK tartrate	0.9 M NaK tartrate	0.9 M NaK tartrate	0.9 M NaK tartrate	0 M NaK tartrate + 10% glycerol
Space group	$P4_12_12$	$P4_12_12$	$P4_12_12$	$P4_12_12$	$P4_12_12$
Unit-cell parameters					
$a = b$ (Å)	57.2	57.9	57.5	57.5	57.7
c (Å)	149.8	149.9	149.5	149.6	149.5
Resolution range (Å)	50.0–1.60 (1.63–1.60)	50.0–1.60 (1.63–1.60)	50.0–1.60 (1.63–1.60)	50.0–1.60 (1.63–1.60)	50.0–1.60 (1.63–1.60)
Unique reflections	34050 (1668)	34268 (1643)	34066 (1673)	34017 (1678)	34268 (1643)
Redundancy	7.1 (6.9)	6.8 (6.5)	7 (5.9)	7 (5.9)	7.1 (7.3)
Completeness (%)	100 (99.9)	98.7 (97.7)	99.9 (100)	99.6 (100)	99.8 (99.3)
R_{sym}‡ (%)	11.1 (57.9)	15.4 (77.4)	6.3 (14.4)	5.7 (11.5)	7.8 (13.0)
$\langle I/\sigma(I)\rangle$	19.7 (3.0)	13.1 (2.0)	30.3 (11.5)	32.4 (14.1)	27.2 (14.4)
Mosaicity (°)	0.67	0.34	0.11	0.12	0.08

† Data sets were taken from the same crystal as shown in Figs. 1(d)–1(e) and Figs. 2(c)–2(d).   ‡ $R_{sym} = \sum |I - \langle I\rangle|/\sum\langle I\rangle$.

of 1.5%. The X-ray beam was collimated to 100×100 μm diameter, yielding a flux of approximately 5×10^{10} photons per second on the sample. In addition to beam-defining slits, guard slits placed 445 mm downstream (Advanced Design Consulting, Lansing, NY, USA, STL-100 series High Precision Slits) served to remove unwanted parasitic scatter. Samples were centered in the beam with a combination of visual positioning (using a perpendicular video camera) and scanning in the X-ray beam while monitoring transmitted beam intensity. Two 7.5 μm-thick polyimide windows (Chemplex Industries, Palm City, FL, USA, catalogue No. 440) provided a 25 mm air gap in the vacuum flight path in which to mount the samples. A 700 series Cryostream (Oxford Cryosystems, Oxford, UK) was used to keep samples at the specified cryogenic temperatures. Images were collected on a PILATUS 100K-S detector (DECTRIS, Baden, Switzerland). The sample-to-detector distance and beam center were calibrated using silver behenate powder ($d_{001} = 58.376$ Å; The Gem Dugout, State College, PA, USA) (Huang *et al.*, 1993). Images were reduced to scattering profiles using the *BioXTAS RAW* software (Nielsen *et al.*, 2009). All images were exposed for 10 s and normalized on the basis of transmitted beam intensity as measured at the beamstop photodiode. Final profiles were obtained by subtracting the normalized empty-cell (air + nitrogen cold stream) signal from the normalized full-cell signal.

3. Results and discussion

Fig. 2 shows diffraction images of high-pressure cryocooled crystals prepared by the three hydration methods. The diffraction image of a crystal obtained using the oil-coating method (Fig. 2a) shows diffuse scatter around 5.5 Å from the coating oil. The diffraction image of a crystal from the capillary-hydration method (Fig. 2b) shows three strong diffuse rings. The innermost diffuse ring (~5.0 Å) is generated from the polycarbonate capillary and the second (~3.0 Å) and third (~2.0 Å) diffuse rings are from the solution inside the capil-

lary. The diffraction images of crystals prepared with the capillary-shielding method (Figs. 2c–2e) produce dramatically reduced background scattering compared to the other hydration methods. The diffraction image (Fig. 2c) from the crystal (Fig. 1d) still within the shielding capillary generates faint background scattering mainly from two different sources: the polyester capillary and a small amount of external and internal solvent from the crystal. When the enclosing polyester capillary is removed, the crystal (Fig. 1e) produces a diffraction image with even less diffuse scattering background (Fig. 2d). It still shows faint diffuse scattering around 3.0 Å, which is from the small amount of solvent internal to and coating the crystal. However, this level of diffuse scattering is comparable to the level of air scattering around the beamstop. The diffuse scattering from the external solvent could perhaps be further reduced by using an adaptation of one of the recently developed mounting techniques (Kitago *et al.*, 2005; Kitatani *et al.*, 2008; Sugahara, 2012).

Diffraction quality was compared by processing complete data sets from thaumatin crystals prepared by the three hydration methods, as shown in Table 1. We observed that the crystals prepared by oil coating produced much higher mosaicity (0.67°) than those produced by the other two methods. We suggest that this could be due to the aggressive mechanical manipulation needed to remove external mother liquor during the oil-coating process. With more gentle treatment during oil coating, we typically observe that the high-pressure cryocooled thaumatin crystals show crystal mosaicity of ~0.2 to 0.4°. Because of this high mosaicity (0.67°) and the relatively high background from the coating oil, the R_{sym} value and the signal-to-noise [$I/\sigma(I)$] ratio are relatively poor (Table 1).

A data set from a crystal prepared by capillary hydration shows a reasonable mosaicity (0.34°) but, because of the high diffuse scattering background and the small crystal size (<100 μm) compared to the capillary size (outside diameter = 300 μm, inside diameter = 200 μm), the R_{sym} value and the signal-to-noise [$I/\sigma(I)$] ratio remain relatively poor. Using the

capillary-shielding method, we first observe that the crystals produce exceptionally good crystal mosaicity (0.08–0.12°). Remarkably, the ten different thaumatin crystals (data from only two crystals are shown in Table 1) prepared by the capillary-shielding method had an average crystal mosaicity of 0.11°, which is very close to the mosaicity (∼0.08°) of unfrozen thaumatin crystals at room temperature. A longer exposure (30 s as opposed to 1 s) showed diffraction spots at 0.93 Å and beyond, approaching the highest diffraction resolution (0.94 Å) reported for thaumatin crystals (Asherie *et al.*, 2009). This indicates that the crystal damage during the capillary-shielding procedure was minimized and crystal cryopreservation was almost ideally performed.

The crystals prepared by capillary shielding (Table 1) show a much improved R_{sym} value and signal-to-noise [$I/\sigma(I)$] ratio. The most dramatic difference was observed in the highest resolution shell (1.63–1.60 Å). This enhancement was due to the dramatically reduced background scattering and improved crystal cryoprotection of the capillary-shielding method. The shielding polyester capillary produces a faint but noticeable diffuse scattering (Figs. 1*d* and 2*c*). When the polyester capillary was removed (Fig. 1*e*), the level of diffuse scattering was further decreased (Fig. 2*d*); this contribution to the data quality improvement can be clearly seen by comparing columns 3 and 4 of Table 1.

Each crystal-hydration method addressed in this study has pros and cons. The oil-coating method is simple and easily applicable for crystals grown by hanging/sitting-drop and oil-batch methods. The method can eliminate most of the outside mother liquor. This process proved to be helpful in suppressing ice formation inside protein crystals even at ambient pressure when the solvent content of the crystal is moderate or low (Kwong & Liu, 1999; Warkentin & Thorne, 2009). Using the oil-coating method followed by high-pressure cryocooling, we found that the solvent inside crystals can be successfully vitrified even in challenging cases. For example, thaumatin crystals can be equilibrated in deionized water for a few hours and pressure cryocooled without losing diffracting power (Kim *et al.*, 2011). We found that, as the salt concentration decreased from the growth condition (0.9 *M*) to 0 *M*, it became more challenging to suppress ice formation with oil coating at ambient pressure. However, we have shown that thaumatin crystals equilibrated in deionized water can be successfully high-pressure cryocooled without adding penetrating cryoprotectants using the oil-coating method (Kim *et al.*, 2011). In such cases, oil coating is the most appropriate hydration method for high-pressure cryocooling; capillary hydration and capillary shielding are inappropriate because pure water around the crystal cannot be easily vitrified even under high pressure.

On the other hand, the oil-coating process is not suitable for very fragile and delicate crystals, as these crystals can be easily damaged during elimination of external mother liquor around the crystal. We also found that oil does not cover crystals properly when the crystals are grown in solutions containing 2-methyl-2,4-pentanediol and polyethylene glycol (PEG). For these crystals, we observed that oil slips off the crystal surface,

exposing the crystal to air and drying the crystal out. Finally, we found that some crystals are unstable and lose diffracting power in oil. When detergents are present in the crystallization solution, the crystals may be unstable in oil; this possibility must be tested before using oil coating as a crystal-hydration method.

The capillary-hydration method is efficient for delicate protein crystals. Once grown in a capillary, crystals are completely protected by the enclosing capillary during handling, therefore eliminating direct physical handling damage to the crystal. This method is also very useful for crystal screening and high-throughput crystallography. As shown in Fig. 1(*b*), many crystals can be grown inside the capillary and can be simultaneously subjected to high-pressure cryocooling for X-ray data collection. On the other hand, as shown in Fig. 2(*b*), the enclosing capillary and the relatively large volume of mother liquor around the crystal produce relatively high background. Therefore, this method is not suitable for tiny and very weakly diffracting crystals. Additionally, water vitrification is challenging with this hydration method. In the cases where protein crystals are grown with sufficient amounts of cryoprotecting chemicals, capillary samples can be successfully pressure cryocooled without additional chemical cryoprotectants. However, when crystals are grown in a very dilute solution, high pressure alone may not suppress ice formation. This problem can be overcome by adding a minimal amount of cryoprotectant into the capillary mother liquor. We showed that adding 10–15%(*v*/*v*) chemical cryoprotectants (*e.g.* glycerol, PEG) into pure water in a polycarbonate capillary (outside diameter = 900 µm, inside diameter = 300 µm) is enough to successfully suppress ice crystallization under pressure (Chen *et al.*, 2009).

The capillary-shielding method should be efficient for tiny or very weakly diffracting crystals. As shown in Figs. 2(*d*)–2(*e*), the method produces very low background. Furthermore, as shown in Table 1, the diffraction quality [in terms of R_{sym}, $I/\sigma(I)$, crystal mosaicity] was exceptionally good and showed almost no sign of crystal damage during crystal handling and cryocooling. On the other hand, this method requires more delicate sample manipulations before high-pressure cryocooling than either the oil-coating or capillary-hydration methods.

As shown in Fig. 1(*e*), with capillary shielding, a small amount of excess mother liquor remains around the crystals. When a crystal is grown in very dilute solution, ice crystallization may not be fully suppressed around the crystal during high-pressure cryocooling. In this case, a small amount of cryoprotectant can be added to the crystal before capillary shielding. As discussed above, the thaumatin crystal equilibrated to deionized water cannot be easily cryocooled with capillary shielding, since pure water around the crystal does not easily vitrify. To overcome this problem, we added 10%(*v*/*v*) glycerol to the thaumatin crystals equilibrated in deionized water and applied high-pressure cryocooling to the crystals using the capillary-shielding method (Fig. 1*f*). Fig. 2(*e*) shows the diffraction image from the sample, which is of exceptional quality. When the crystal was quickly thawed to room

temperature for a few seconds and frozen back to 100 K in the N₂ cold stream (Fig. 1g), it produced strong hexagonal ice rings with very poor crystal diffraction (Fig. 2f), showing that
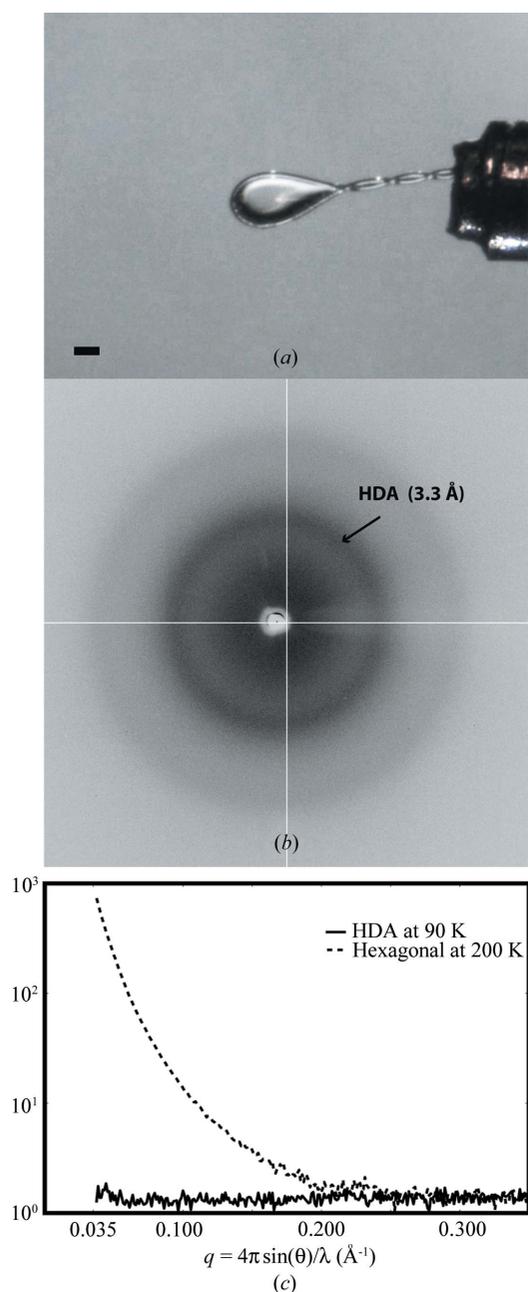
Figure 3
Test of solvent film for X-ray diffraction microscopy. (a) Test solution, 10%(v/v) glycerol/water in a cryoloop, high-pressure cryocooled at 200 MPa using the capillary-shielding method. The film, which is about 10 μm thick, looks transparent. The scale bar indicates 100 μm. (b) X-ray scattering (in the wide-angle regime) from the sample at 100 K, confirming that the water film was vitrified. The central peak position (3.3 Å) of the primary diffuse scattering indicates that HDA ice is present. (c) SAXS profiles from a 1 mm-thick high-pressure cryocooled sample of 15%(v/v) glycerol/water solution. Solid line, at 90 K. Dashed line, after warming to 200 K. The uniform and flat profile indicates that the high-density amorphous ice induced by high-pressure cryocooling is homogeneous in the given q range (0.035–0.35 Å⁻¹). At 200 K, the HDA ice has transformed to hexagonal ice, with a dramatically increased non-uniform profile, indicating increased local density fluctuations in the 1.8–18 nm range. SAXS profiles have been scaled to match the high-q regions.

high pressure had successfully cryoprotected this sample. This example demonstrates that even challenging crystals (*i.e.* crystals having high solvent content and large solvent channels or grown in dilute solution) may be successfully high-pressure cryocooled by the capillary-shielding method with the addition of small amounts of cryoprotectant.

Beyond the cryoprotection of protein crystals, the capillary-shielding method has great potential in cryopreserving noncrystalline hydrated biological samples for coherent X-ray diffraction imaging. For example, X-ray diffraction microscopy (XDM) of frozen–hydrated samples (Huang *et al.*, 2009; Lima *et al.*, 2009) is an emerging microscopy technique for wet, intact, micrometre-sized biological samples that fills the resolution gap between optical microscopy and transmission electron microscopy. However, preserving biological samples in an amorphous ice layer suitable for XDM has been a challenge (Sayre, 2008). For successful image reconstruction, the diffraction patterns from a sample should be adequately oversampled, which is achieved by having a clean background around the sample. When the biological sample is frozen in a solution film at ambient pressure, the supporting amorphous ice layer may be contaminated with the microcrystalline ice, which would register as another scattering object. To address this problem, the capillary-shielding method can be employed to create an amorphous ice layer under high pressure. A test using a water solution [10% glycerol (v/v) solution, ~10 μm thickness] in a nylon loop (Fig. 3a) showed diffraction (Fig. 3b), indicating that the water solution had been successfully cryocooled to form high-density amorphous ice. A SAXS profile shows that the high-density amorphous ice induced by high-pressure cryocooling produces a very uniform and flat background in the q range of 0.035–0.35 Å⁻¹ (Fig. 3c), which confirms the homogeneity of high-density amorphous ice and lack of crystalline ice contamination. Thus, capillary shielding and the high-pressure cryocooling method could be extended to preserve hydrated biological samples in an amorphous layer, which might increase the success rate of XDM reconstructions.

4. Conclusion

In this study, we have demonstrated a new crystal-hydration method, capillary shielding, for high-pressure cryocooling. Using the method, a protein crystal can be properly high-pressure cryocooled with little or no added cryoprotectant, and improved X-ray diffraction data can be obtained with significantly reduced background scattering. Along with the two existing crystal-hydration methods, oil coating and capillary hydration, the new hydration method extends the range of applicability of high-pressure cryocooling in macromolecular crystallography. The oil-coating method is effective for crystals that are grown in a dilute solution and are unstable against even slight chemical changes in the crystallization solution. The capillary-hydration method is useful for crystals that are sensitive to physical handling, and for high-throughput screening and data collection. The capillary-shielding method

is useful for crystals that are weakly diffracting and/or are easily damaged by conventional cryoprotection procedures.

The newly developed method also allows increased application of high-pressure cryocooling to other cases where sample cryoprotection is required. Examples include electron microscopy and coherent X-ray diffraction imaging of fully hydrated and typically noncrystalline biological samples. The high-density amorphous ice formed by high-pressure cryocooling ensures clean background support without crystalline ice contamination. High-pressure cryocooling using the capillary-shielding method may serve as a useful sample cryopreservation technique for diffraction imaging of biological samples using the ultra-bright coherent X-ray beams from the next generation of X-ray sources, such as X-ray free-electron lasers and energy-recovery linacs (Bilderback *et al.*, 2010).

References

Albright, R. A., Ibar, J. L. V., Kim, C. U., Gruner, S. M. & Morais-Cabral, J. H. (2006). *Cell*, **126**, 1147–1159.

Alcorn, T. & Juers, D. H. (2010). *Acta Cryst.* D**66**, 366–373.

Asherie, N., Jakoncic, J., Ginsberg, C., Greenbaum, A., Stojanoff, V., Hrnjez, B. J., Blass, S. & Berger, J. (2009). *Cryst. Growth Des.* **9**, 4189–4198.

Barstow, B., Ando, N., Kim, C. U. & Gruner, S. M. (2008). *Proc. Natl Acad. Sci. USA*, **105**, 13362–13366.

Barstow, B., Ando, N., Kim, C. U. & Gruner, S. M. (2009). *Biophys. J.* **97**, 1719–1727.

Bilderback, D. H., Brock, J. D., Dale, D. S., Finkelstein, K. D., Pfeifer, M. A. & Gruner, S. M. (2010). *New J. Phys.* **12**, 035011.

Bujacz, G., Wrzesniewska, B. & Bujacz, A. (2010). *Acta Cryst.* D**66**, 789–796.

Chen, Y.-F., Tate, M. W. & Gruner, S. M. (2009). *J. Appl. Cryst.* **42**, 525–530.

Chinte, U., Shah, B., DeWitt, K., Kirschbaum, K., Pinkerton, A. A. & Schall, C. (2005). *J. Appl. Cryst.* **38**, 412–419.

Dewan, J. C. & Tilton, R. F. (1987). *J. Appl. Cryst.* **20**, 130–132.

Domsic, J. F., Avvaru, B. S., Kim, C. U., Gruner, S. M., Agbandje-McKenna, M., Silverman, D. N. & Mckenna, R. (2008). *J. Biol. Chem.* **283**, 30766–30771.

Garman, E. (1999). *Acta Cryst.* D**55**, 1641–1653.

Garman, E. (2003). *Curr. Opin. Struct. Biol.* **13**, 545–551.

Garman, E. F. & Doublie, S. (2003). *Methods Enzymol.* **368**, 188–216.

Garman, E. F. & Mitchell, E. P. (1996). *J. Appl. Cryst.* **29**, 584–587.

Garman, E. F. & Owen, R. L. (2006). *Acta Cryst.* D**62**, 32–47.

Garman, E. F. & Schneider, T. R. (1997). *J. Appl. Cryst.* **30**, 211–237.

Haas, D. J. & Rossmann, M. G. (1970). *Acta Cryst.* B**26**, 998–1004.

Henderson, R. (1990). *Proc. R. Soc. London Ser. B*, **241**, 6–8.

Hope, H. (1988). *Acta Cryst.* B**44**, 22–26.

Huang, T. C., Toraya, H., Blanton, T. N. & Wu, Y. (1993). *J. Appl. Cryst.* **26**, 180–184.

Huang, X. J., Nelson, J., Kirz, J., Lima, E., Marchesini, S., Miao, H. J., Neiman, A. M., Shapiro, D., Steinbrener, J., Stewart, A., Turner, J. J. & Jacobsen, C. (2009). *Phys. Rev. Lett.* **103**, 198101.

Juers, D. H. & Matthews, B. W. (2004). *Q. Rev. Biophys.* **37**, 105–119.

Kalinin, Y., Kmetko, J., Bartnik, A., Stewart, A., Gillilan, R., Lobkovsky, E. & Thorne, R. (2005). *J. Appl. Cryst.* **38**, 333–339.

Kim, C. U., Barstow, B., Tate, M. W. & Gruner, S. M. (2009). *Proc. Natl Acad. Sci. USA*, **106**, 4596–4600.

Kim, C. U., Chen, Y.-F., Tate, M. W. & Gruner, S. M. (2008). *J. Appl. Cryst.* **41**, 1–7.

Kim, C. U., Hao, Q. & Gruner, S. M. (2006). *Acta Cryst.* D**62**, 687–694.

Kim, C. U., Hao, Q. & Gruner, S. M. (2007). *Acta Cryst.* D**63**, 653–659.

Kim, C. U., Kapfer, R. & Gruner, S. M. (2005). *Acta Cryst.* D**61**, 881–890.

Kim, C. U., Tate, M. W. & Gruner, S. M. (2011). *Proc. Natl Acad. Sci. USA*, **108**, 20897–20901.

Kitago, Y., Watanabe, N. & Tanaka, I. (2005). *Acta Cryst.* D**61**, 1013–1021.

Kitatani, T., Sugiyama, S., Matsumura, H., Adachi, H., Yoshikawa, H. Y., Maki, S., Murakami, S., Inoue, T., Mori, Y. & Takano, K. (2008). *Appl. Phys. Express*, **1**, 037002.

Ko, T.-P., Day, J., Greenwood, A. & McPherson, A. (1994). *Acta Cryst.* D**50**, 813–825.

Kriminski, S., Caylor, C. L., Nonato, M. C., Finkelstein, K. D. & Thorne, R. E. (2002). *Acta Cryst.* D**58**, 459–471.

Kwong, P. D. & Liu, Y. (1999). *J. Appl. Cryst.* **32**, 102–105.

Lima, E., Wiegart, L., Pernot, P., Howells, M., Timmins, J., Zontone, F. & Madsen, A. (2009). *Phys. Rev. Lett.* **103**, 198102.

Low, B. W., Chen, C. C., Berger, J. E., Singman, L. & Pletcher, J. F. (1966). *Proc. Natl Acad. Sci. USA*, **56**, 1746–1750.

Mueller-Dieckmann, C., Kauffmann, B. & Weiss, M. S. (2011). *J. Appl. Cryst.* **44**, 433–436.

Nielsen, S. S., Toft, K. N., Snakenborg, D., Jeppesen, M. G., Jacobsen, J. K., Vestergaard, B., Kutter, J. P. & Arleth, L. (2009). *J. Appl. Cryst.* **42**, 959–964.

Otwinowski, Z. & Minor, W. (1997). *Methods Enzymol.* **276**, 307–326.

Petsko, G. A. (1975). *J. Mol. Biol.* **96**, 381–392.

Pflugrath, J. W. (2004). *Methods*, **34**, 415–423.

Ravelli, R. B. G. & McSweeney, S. M. (2000). *Struct. Fold. Des.* **8**, 315–328.

Riboldi-Tunnicliffe, A. & Hilgenfeld, R. (1999). *J. Appl. Cryst.* **32**, 1003–1005.

Rodgers, D. W. (1994). *Structure*, **2**, 1135–1140.

Rodgers, D. W. (1997). *Methods Enzymol.* **276**, 183–203.

Sayre, D. (2008). *Acta Cryst.* A**64**, 33–35.

Schneider, T. R. (1997). *Acta Phys. Pol. A*, **91**, 739–744.

Sugahara, M. (2012). *J. Appl. Cryst.* **45**, 362–366.

Teng, T.-Y. & Moffat, K. (1998). *J. Appl. Cryst.* **31**, 252–257.

Urayama, P., Phillips, G. N. & Gruner, S. M. (2002). *Structure*, **10**, 51–60.

Warkentin, M., Berejnov, V., Husseini, N. S. & Thorne, R. E. (2006). *J. Appl. Cryst.* **39**, 805–811.

Warkentin, M. & Thorne, R. E. (2009). *J. Appl. Cryst.* **42**, 944–952.